UCRL-JRNL-202168

LAWRENCE
LIVERMORE
NATIONAL
LABORATORY

Monte Carlo Models for the Production of β-delayed Gamma Rays Following Fission of Special Nuclear Materials

J. Pruet, J. Hall, M.-A. Descalle, S. Prussin

February 6, 2004

Nuclear Instruments and Methods

Disclaimer

This document was prepared as an account of work sponsored by an agency of the United States Government. Neither the United States Government nor the University of California nor any of their employees, makes any warranty, express or implied, or assumes any legal liability or responsibility for the accuracy, completeness, or usefulness of any information, apparatus, product, or process disclosed, or represents that its use would not infringe privately owned rights. Reference herein to any specific commercial product, process, or service by trade name, trademark, manufacturer, or otherwise, does not necessarily constitute or imply its endorsement, recommendation, or favoring by the United States Government or the University of California. The views and opinions of authors expressed herein do not necessarily state or reflect those of the United States Government or the University of California, and shall not be used for advertising or product endorsement purposes.

Monte Carlo Models for the Production of β-delayed Gamma Rays Following Fission of Special Nuclear Materials

J. Pruet [a,*], J. Hall [b], M.-A. Descalle [c], S. Prussin [d]

[a] *Lawrence Livermore National Laboratory, N-Division, L-414 Livermore, CA 94550*

[b] *Lawrence Livermore National Laboratory, N-Division, L-050, Livermore, CA 94550*

[c] *Lawrence Livermore National Laboratory, M-Division, L-174, Livermore, CA 94550*

[d] *Department of Nuclear Engineering, University of California at Berkeley, CA 94720*

Abstract

A Monte Carlo method for the estimation of β-delayed γ-ray spectra following fission is described that can accomodate an arbitrary time-dependent fission rate and photon collection history. The method invokes direct sampling of the independent fission yield distributions of the fissioning system, the branching ratios for decay of individual fission products and the spectral distributions for photon emission for each decay mode. Though computationally intensive, the method can provide a detailed estimate of the spectrum that would be recorded by an arbitrary spectrometer, and can prove useful in assessing the quality of evaluated data libraries, for identifying gaps in these libraries, etc. The method is illustrated by a first comparison of calculated and experimental spectra from decay of short-lived fission products following the reactions $^{235}\mathrm{U}(\mathrm{n_{th}},\mathrm{f})$ and $^{239}\mathrm{Pu}(\mathrm{n_{th}},\mathrm{f})$. For general purpose transport calculations, where detailed consideration of the large number of individual γ-ray transitions in a spectrum may be unnecessary, it is shown that an accurate and simple parameterization of a γ-ray source function can be obtained. These parametrizations should provide high-quality average spectral distributions that should prove useful in calculations describing photons escaping from thick attenuating media.

Key words: Monte Carlo Simulations, Fission reactions
PACS: 24.10.Lx, 25.85.-w

1 Introduction

During the past few years there has been increasing interest in the development of methods for the detection of clandestine fissionable material that may be hidden in sea-going cargo containers (see [1] and references contained therein). Recent work by Norman, *et al.* [2] has demonstrated that the relatively intense, high-energy ($E_\gamma \geq 2.5$MeV) delayed γ-rays emitted during the decay of short-lived fission products might prove to be a useful signature for detection of such material in the presence of thick hydrogenous and other cargoes. This, in turn, has identified the need to find a way to predict delayed γ-ray spectra under a variety of fission rate histories and incorporate these spectra into Monte Carlo codes in order to assess their transport characteristics through a wide range of cargo compositions and geometries.

In this paper we describe a straightforward Monte Carlo approach that provides estimates of the delayed γ-ray spectra produced following a single fission, or for any arbitrary fission rate and photon collection history. This method is based on direct sampling of evaluated independent fission yield distributions and evaluated decay properties of the individual fission products. As a first test of the method, we have compared our calculated spectra with those obtained by Norman, *et al.*

The spectrum of delayed γ-rays from decay of an arbitrary short-lived ($t_{1/2} \leq$1-2 min) fission product tends to be composed of a large number of transitions, each with relatively small absolute intensity per decay. This is especially true of the high-energy (2.5MeV $\leq E_\gamma \leq$ 8MeV) portion of the spectrum. As a result, the delayed γ-ray spectrum from decay of a collection of short-lived fission products will be very complex indeed. Recognizing that attenuation coefficients for photons in essentially all materials over this energy range are only weakly dependent on energy, there is no real need, in the general case, to incorporate the highly-detailed delayed γ-ray source spectrum into a Monte Carlo code in order to assess the effects of different attenuating media and geometries on transmitted spectra. For this purpose, we demonstrate that simple parametric fits to the Monte Carlo source spectra provide high-quality, time-dependent, energy-averaged distributions that can be incorporated into general photon transport calculations.

* Corresponding author. tel: (925) 243-1219
Email address: `pruet1@llnl.gov` (J. Pruet).

2 Monte Carlo Calculations of Delayed γ-ray Spectra

The basic quantity we wish to derive is the delayed γ-ray source function. This function describes the production of photons following spontaneous or induced fission and can be written as

$$s_\gamma(E_\gamma, t) \equiv \frac{d^2 n_\gamma}{dt dE_\gamma}(E_\gamma, t). \tag{1}$$

Here E_γ is the energy of the delayed photon, t is the time at which the photon is emitted following fission and, for the case of induced fission, s_γ is understood to be a function of the energy of the fission-inducing particle. Once s_γ has been determined, the spectrum for any fission rate and decay (counting) history can be determined.

Using neutron-induced fission as an example, a specific binary fission event and the subsequent decays of the fission fragments and their progeny can be expressed as

$$\mathrm{n} +^{\mathrm{A}} \mathrm{Z} \rightarrow \left[\begin{array}{c} {}^{\mathrm{A}_1}\mathrm{Z}_1 \rightarrow^{\mathrm{A}_1^*} (\mathrm{Z}_1 + 1) \rightarrow^{\mathrm{A}_1} (\mathrm{Z}_1 + 1) \rightarrow^{\mathrm{A}_1} (\mathrm{Z}_1 + 2)... \\ {}^{\mathrm{A}_2}\mathrm{Z}_2 \rightarrow^{\mathrm{A}_2 - 1} (\mathrm{Z}_2 + 1) + \mathrm{n} \rightarrow^{\mathrm{A}_2 - 1} (\mathrm{Z}_2 + 2)... \end{array} \right. . \tag{2}$$

Here ${}^{\mathrm{A}}\mathrm{Z}$ is the target nucleus and ${}^{\mathrm{A_i}}\mathrm{Z_i}$ (i=1,2) represent the fission fragments following emission of prompt radiation but before β-decay or isomeric transitions have taken place. We indicate explicitly in Eq. (2) that the nuclides which we are dealing with may be isomers or β-delayed neutron emitters by the decay of the products ${}^{\mathrm{A}_1}\mathrm{Z}_1$ and ${}^{\mathrm{A}_2}\mathrm{Z}_2$, respectively.

The calculation proceeds by randomly choosing a fission product and its decay time following fission and weighting by its independent fission yield and lifetime. For each decay, the energy of an emitted photon is chosen randomly from the known spectrum of photons emitted following its decay and the event weighted according to the absolute intensity of the photon. We do not follow photon cascades directly; rather, we assume that the proper spectral distribution will be reproduced statistically by sampling of individual photons from the known spectrum. Daughter production is determined by sampling from known branching ratios in the decay of the nuclide. Photon emission from decay of the daughter is determined in the same way that photon emission from the parent is determined. The process is repeated for each of the progeny until, in the present case, a nuclide with $t_{1/2} > 10^7$sec is produced.

The calculation of s_γ can be fairly lengthy because of the very large number of nuclides and γ-rays involved. For example, the independent yield evaluations of England and Rider [3] and the nuclide decay properties contained in the

NuDat [1] nuclear data files provide data for some 1000 nuclides, 100 isomers and 20,000 discrete $\gamma-$ray transitions. Nevertheless, the Monte Carlo development of a delayed γ-ray spectrum in histogram form with bin widths of 1 keV that includes decay times in the range $0 \leq t \leq 100$ sec following fission (and which possesses reasonable statistics for the more intense high-energy photons) takes only about ten minutes on a 3-GHz single-processor desktop PC. In the next section, calculations intended to approximately reproduce the irradiation and counting history of the experiments done by Norman, *et al.* are discussed. These calculations have about 3 times better statistical quality (i.e. about ten times more counts per line) than the Norman, *et al.* experiments and took about 40 minutes to run.

3 Comparison with experiment

Although more detailed benchmark experiments have yet to be carried out, we can get an initial estimate of how well our calculations compare with experiment by referring to the measurements reported by Norman, *et al.*. In these experiments, targets of ^{235}U (93% isotopic abundance) and ^{239}Pu (95% isotopic abundance) were exposed to a well-thermalized neutron flux for a period of 30 sec. Following this, the samples were counted with an 80% relative efficiency HPGe detector for 30 sec. The counting period was divided into 10 successive 3-sec periods to follow the decay of individual lines. The transit time between the irradiation and counting sites was about 2.5 sec. To acquire reasonable statistics, some 20 irradiation/counting cycles were performed for each target. The time between each successive irradiation/counting cycle was approximately 1-2 min.

The data files on which our test calculations are based are those of England and Rider and NuDat as noted above. We have assumed that the time after the end of a counting interval and the start of the next irradiation is 100 sec and we have taken the transit time to be 3 sec. A significant complication in calculating estimates of HPGe spectra is the fact that the relative and absolute efficiency functions for the detector used in the experiments of Norman, *et al.* are not well known. Further, the axis of the detector was perpendicular to the source-detector distance rather than facing the source (on axis) as might normally be expected. Also, the geometry of shielding material was fairly complex. As a result, we attempt to compare the predicted and experimental spectral distributions using the relative full-energy, single-escape and double-escape peak efficiency functions calculated by Owens, *et al.* [4] for a 7 cm (diameter) $\times$ 7 cm (length) Ge detector. This detector has a volume close to

[1] NuDat is a web-based nuclear data archive that contains easily readable data taken from ENSDF files. The URL is http://www.nndc.bnl.gov/nndc/nudat/ .

that of the detector actually used in the Norman, *et al.* experiment. Spectral magnitudes were normalized by reference to a strong, well-isolated line of known intensity. We note that the calculations of Owens, *et al.* are also for a source on axis with the detector and thus the energy dependence of the efficiency functions cannot be expected to reproduce the experiment exactly. A rough estimate of the uncertainty implied by our use of the calculations in Owens, *et. al* is obtained by reference to the efficiency functions reported by these authors for a 5 cm (diameter) $\times$ 5 cm (length) HPGe detector. For this smaller detector, the calculated full-energy peak efficiencies at $E_\gamma = 2$ MeV, 3 MeV, and 5 MeV, relative to that at $E_\gamma = 1$ MeV, are smaller than the corresponding ratios for the 7 cm (diameter) x 7 cm (length) detector by 14%, 20% and 30%, respectively. These considerations imply uncertainties of about $20 - 30\%$ in our simple estimates of the full-energy peak efficiency at high energies.

Normalization of the calculated and experimental spectra was obtained with the full-energy peak at 1427 keV. This line is attributed to the decay of ^{94}Sr ($t_{1/2} = 75.3\,\mathrm{sec}$), which is sufficiently long-lived that timing uncertainties on the order of 1 sec in the beginning of a count are not significant. Further, the ^{94}Rb ($t_{1/2} = 2.70\,\mathrm{sec}$) precursor of this nuclide is sufficiently short-lived that uncertainties associated with precursor decay are also not significant. Finally, the independent and cumulative fission yields of ^{94}Sr have rather small uncertainties ($\leq 6\%$) in the thermal fission of ^{239}Pu and the uncertainties are even smaller for thermal fission of ^{235}U. The actual normalization was accomplished by comparing peak intensities at 1427 keV in the 3-sec spectrum from ^{235}U and ^{239}Pu that began at $t_0 = 15\,\mathrm{sec}$ following the end of irradiation.

To proceed with a comparison between calculations and experiment, let $r(E_\gamma)$ represent the line spectrum incident upon the HPGe detector under experimental conditions, $o(E_\gamma)$ the complete spectrum registered by the detector, and let $m(E_\gamma)$ represent the line spectrum estimated from the Monte Carlo calculation. In the absence of all errors, the ratio $m(E_\gamma)/r(E_\gamma)$ should be a constant. The functions $o(E_\gamma)$ and $r(E_\gamma)$ are related by

$$\begin{aligned} o(E_\gamma) = \epsilon_{\mathrm{fep}}(E_\gamma) r(E_\gamma) + \epsilon_1(E_\gamma + m_e c^2) r(E_\gamma + m_e c^2) \\ + \epsilon_2(E_\gamma + 2m_e c^2) r(E_\gamma + 2m_e c^2) + b(E_\gamma), \end{aligned} \tag{3}$$

where ϵ_{fep}, ϵ_1 and ϵ_2 represent the full-energy, single-escape and double-escape peak efficiencies, respectively, and $b(E_\gamma)$ represents the continuum from the interaction of photons with energy E_γ.

Equation 3 then implies that a comparison of the calculated quantity $\langle o(E_\gamma) -$

$b(E_\gamma)\rangle$, estimated from the experimental data, with the quantity

$$\begin{aligned}\langle \epsilon_{\rm fep}(e_{E_\gamma})m(E_\gamma) + \epsilon_1(E_\gamma + m_e c^2)m(E_\gamma + m_e c^2) \\ +\epsilon_2(E_\gamma + 2m_e c^2)m(E_\gamma + 2m_e c^2)\rangle\end{aligned} \tag{4}$$

obtained from Monte Carlo calculations should provide a reasonable first estimate of a quantitative comparison between calculation and experiment. The averaging implied by the brackets could be over any desired energy interval. For the present case, we estimated averages over individual lines or unresolved multiplets in the experimental spectrum. Adjacent energy bins with $o(j) - b(j) > 1.5\sigma_b$ (see below) are considered to comprise a single line or unresolved multiplet. The total number of counts in a spectral peak is estimated as the sum of $o(j) - b(j)$ over these bins and the centroid of the peak is estimated as the mean of $E_\gamma(j)(o(j) - b(j))$ for these bins. We note that the experimental measurements were taken with a system gain of approximately 1.1 keV per channel and also that the HPGe displayed a resolution of about 2.0 keV (FWHM) at 1332.5 keV.

The principal issue in obtaining a reasonable comparison between the calculated and experimental line spectra is the estimation of $b(E_\gamma)$. Rather than attempt to calculate this directly from first principles, we use a simple approximation that should suffice for the present purposes. Because a very large number of lines contribute to the experimental spectra, $b(E_\gamma)$ tends to vary smoothly and slowly with energy. Motivated by this observation, we adopt a simple estimate for $b(E_\gamma)$ in the experimental spectra. First, the average number of counts in 50 adjacent energy bins (channels) is calculated as

$$\bar{o} = \frac{1}{50}\sum_{j_0}^{j_0+50} o(j). \tag{5}$$

Here $o(j)$ is the number of counts observed in the jth bin. In the absence of *apriori* information on the fraction of total counts in the summation due to continuum events, we make the arbitrary but conservative assumption that the majority of counts are background counts and thus the uncertainty in the background is approximately $\sigma_b = \sqrt{\bar{o}}$. The average value of the background counts per channel in this channel range, $\bar{b}$, is now estimated as the average number of counts in each bin for which the relation $o(j) - \bar{o} < 2\sigma_b$ is satisfied. This $\bar{b}$ is assigned as $b(j_0 + 25)$. This process is repeated for $j_0 = 0, 50, 100, ...$ until the whole experimental spectrum has been covered. Linear interpolation between the different $b(j_0+25)$ values is used to estimate $b(E_\gamma)$ for an arbitrary energy.

Figures 1 and 2 show comparisons of the type described above for fission of ^{239}Pu and photons collected in the 3 sec bin beginning at $t_0 = 30$ sec following fission. Table 1 gives a comparison between the calculated and experimentally-

determined intensities of prominent γ-rays emitted with $1\text{MeV} < E_\gamma < 5\text{MeV}$ collected in the 3 sec bin beginning at $t_0 = 6\,\text{sec}$ following fission. Figures 3 and 4 show similar comparisons for the spectrum observed following fission of the ^{235}U sample.

Scanning through the table and figures, it is immediately evident that peak distributions and intensities are generally quite similar, although some obvious discrepancies are noted. Some predicted lines in the spectra from both ^{239}Pu and ^{235}U fission products are not observed in the experimental spectra with significant intensity and *vice versa*, and there are some notable discrepancies in the calculated and observed line intensities in some cases. For example, the intensity of lines at energies of 1107 keV and 1750 keV are roughly twice as large in the calculated spectrum for ^{239}Pu at $t_0 = 6\,\text{sec}$ as compared to the experimental spectrum (see Table 1). These lines arise with high intensity in the decay of $^{96\text{m}}\text{Y}(t_{1/2} = 9.6\,\text{sec})$ but are only weak components in the decay of $^{96}\text{Y}(t_{1/2} = 5.34\,\text{sec})$. Isomer ratios in fission have been notoriously difficult to measure or predict over the years and it may be that the ratios suggested by England and Rider need to be adjusted in this case. Such an adjustment would lie well within the uncertainties permitted by the evaluated fission yields.

A detailed comparison between the calculated and the experimental spectra of Norman, *et al.* is clearly unwarranted here because of the complications noted in the above discussion. Nevertheless, we can conclude that the general agreement is reasonable. Also, this method, coupled with accurately modeled benchmark spectra, may be very useful in assessing the general quality of the data bases involved. It may also be possible to improve the quality of the evaluated data files where, at present, very large uncertainties exist.

4 Simple Parametrizations of the γ-ray Source Functions

As noted above, the γ-ray source function obtained directly from the Monte Carlo simulations is generally much too detailed for general purpose transport calculations, especially when shielding materials have thicknesses of a few attenuation mean free paths or more. We have found, as might be expected, that the source functions calculated for delayed γ rays can be quite-well represented by continuous functions of the form

$$s_\gamma(E_1, E_2, t) = A_1 e^{-t/\tau_1} + A_2 e^{-t/\tau_2} + A_3 e^{-t/\tau_3}. \tag{6}$$

Here E_1 and E_2 represent the lower and upper photon energies over which the fitting applies, and all $\tau_i > 0$. Figure 5 shows representative examples of fits over 500-keV intervals to the source functions calculated for $^{239}\text{Pu}(\text{n}_{\text{th}}, \text{f})$. The corresponding fitting parameters are given in Table 2. It is clear from the

figure that the fitting functions represent the source functions quite accurately. Similar quality fits were obtained for the source function for thermal neutrons on ^{235}U. These parameterizations of s_γ should permit relatively rapid transport calculations over a wide range of conditions.

5 Discussion and Conclusions

Complete Monte Carlo simulations of fissioning systems, including nuclide production and decay and transport of their decay radiations are not currently directly possible because the appropriate data libraries are not coupled into the codes. This can be rectified easily and can provide highly detailed simulations in cases where such detail might be warranted as the examples discussed in this paper demonstrate. For the general case of photon transport following an arbitrary fission history, high detail is not warranted and the high accuracy of the parameterized source functions provide a simple route for photon transport calculations that should prove adequate to a wide range of problems.

As with all Monte Carlo calculations, the results obtained are limited by the physics contained in the code being used and the quality of the experimental data contained in the libraries from which the code draws its information. For the most part, the decay properties of the longer-lived fission products have been adequately studied for most applications; however, for the case of cargo interrogation for the presence of clandestine fissionable materials, we must deal with some of the shortest-lived fission products with $\mathrm{Z} \leq \mathrm{Z_p}$ (the most probable atomic number of a fission fragment isobar) where data sets on decay radiations may be incomplete and where estimated uncertainties in independent fission yields are commonly rather large. The adequacy of the evaluated data libraries can only be judged through comparison of detailed benchmark experiments with Monte Carlo calculations. Such benchmark experiments are now in the planning stage at Lawrence Berkeley National Laboratory.

6 Acknowledgments

We thank Ed Lent and Rich Buck of Lawrence Livermore National Laboratory for helpful discussions on implementing delayed gammas in Monte Carlo transport codes.

This work was performed under the auspices of the U.S. Department of Energy by the University of California, Lawrence Livermore National Laboratory under contract W-7405-ENG-48.

References

[1] D. Slaughter, M. Accatino, A. Bernstein, J. Candy, A. Dougan, J. Hall, A. Loshak, D. Manatt, A. Meyer, B. Pohl, S.G. Prussin, R. Walling, & D. Weirup, "Detection of special nuclear material in cargo containers using neutron interrogation", Lawrence Livermore Laboratory Report UCRL-ID-155315, August 2003

[2] E.B. Norman, S.G. Prussin, S.G., R.-M. Larimer, H. Shugart, E. Browne, A. Smith, R.J. McDonald, H. Nitsche, P. Gupta, M. Frank & B. Gosnell "Signatures of Special Nuclear Material: High-Energy γ-rays Folowing Fission", Nuclear Instruments and Methods, in press 2004

[3] T.R. England & B.F. Rider "Evaluation and Compilation of Fission Product Yields", LA-UR-94-3106, ENDF-349, 1994

[4] A. Owens, N. Gehrels, S. Pascarelle, & B.J. Teegarden "Monte-Carlo Calculations of Ge Detector Escape-Peak Efficiencies" 1991, IEEE Transactions on Nuclear Science, 38, 559

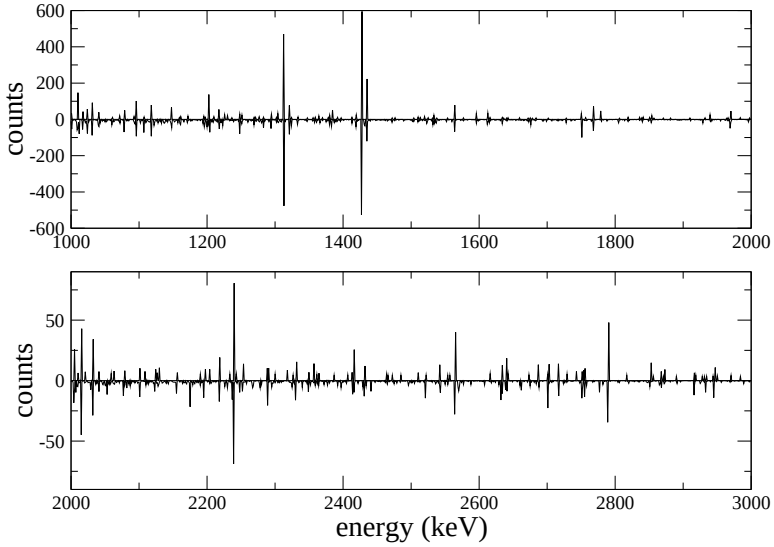

Fig. 1. Comparison between the Norman, *et al.* experiments and the present calculations for thermal neutrons incident on ^{239}Pu and photons collected in the 3 sec bin beginning at $t_0 = 30$ sec following fission. In each panel the experimental line spectrum, including full-energy, single-escape and double escape peaks is shown in the upper half and the corresponding Monte Carlo result is shown in the bottom half multiplied by -1. See text for details.

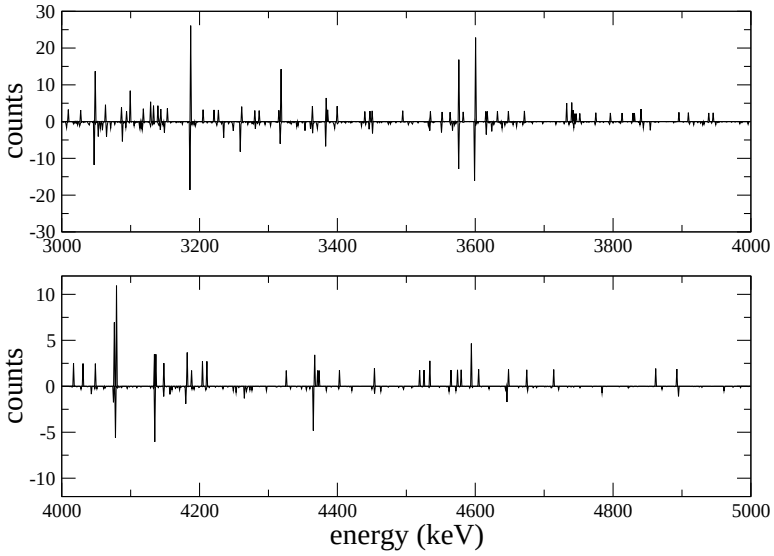

Fig. 2. Same as figure 1 except for photons in the $3 - 5$MeV range.

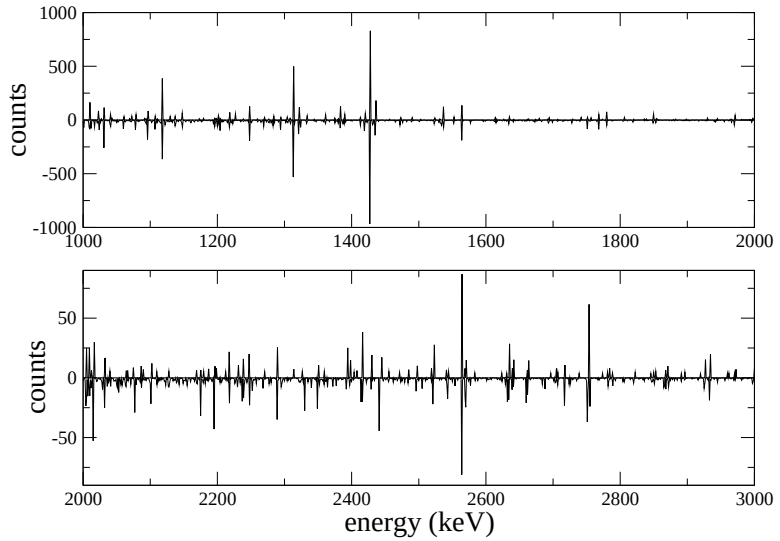

Fig. 3. Same as figure 1 except for thermal neutrons incident on ^{235}U.

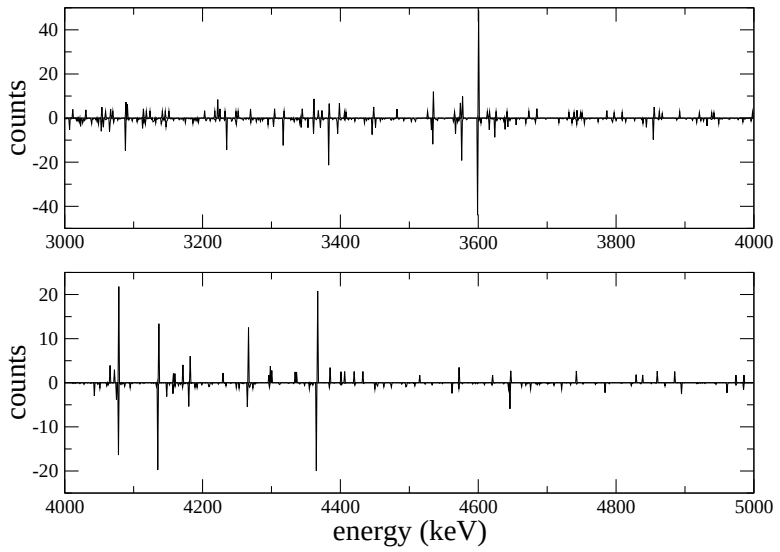

Fig. 4. Same as figure 3 except for photons in the $3 - 5$MeV range.

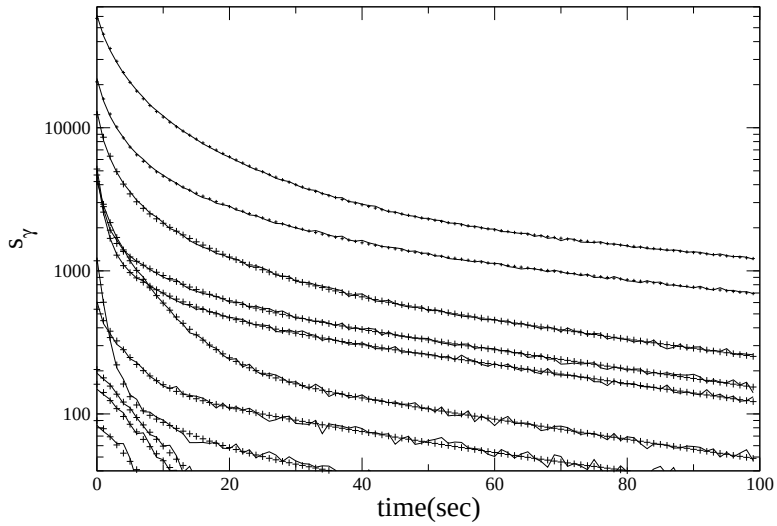

Fig. 5. Comparison of the results of the monte carlo calculation of the photon source function with simple fits to this function based on Eq. (6) for thermal neutron induced fission of ^{239}Pu. The different lines correspond to different energy regions. The top line - highest photon counts - represents the photon source function in the energy range 500-1000 keV, the next line in the range 1000-1500 keV, and so on until the lowest line which represents counts in the 5500-6000 keV range. The thin line corresponds in each case to the output from the Monte Carlo simulation and crosses correspond to the simple fit described by Eq. (6). The units for s_γ here are photons/(sec $\cdot 10^6$fissions $\cdot$ 500keV).

Table 1
Prominent lines in the spectrum from thermal neutrons on ^{239}Pu at $t_0 = 6\,\mathrm{sec}$

energy(keV)	experimental counts [a]	MC counts
1-2MeV		
1427.0	657.4[13.4]	680.6[5.9]
1312.6	587.7[12.0]	614.3[5.4]
1750.3	256.1[5.2]	535.4[4.7]
1107.0	136.6[2.8]	382.8[3.3]
1010.0	233.5[4.8]	225.3[2.0]
1118.0	185.7[3.8]	183.6[1.6]
1022.0	161.9[3.3]	200.7[1.8]
1218.0	207.0[4.2]	128.8[1.1]
1435.0	201.6[4.1]	118.3[1.0]
1278.7	58.2[1.2]	196.2[1.7]
2-3MeV		
2237.0	105.2[10.0]	114.0[5.5]
2789.0	57.5[5.5]	44.4[2.1]
2564.0	31.0[2.9]	34.5[1.7]
2701.0	30.1[2.9]	32.6[1.6]
2012.5	14.1[1.3]	48.5[2.3]
2175.0	36.4[3.5]	24.0[1.1]
2716.7	24.1[2.3]	25.4[1.2]
2330.0	28.0[2.7]	19.6[0.9]
2945.0	27.0[2.6]	19.4[0.9]
2077.0	17.3[1.6]	27.7[1.3]
2247.2	20.8[2.0]	24.0[1.1]
3-4MeV		
3287.0	20.0[5.9]	54.5[10.3]
3188.2	45.0[13.4]	0.0[0.0]
3399.7	3.8[1.1]	39.4[7.5]
3599.0	11.8[3.5]	20.1[3.8]
3259.0	16.4[4.9]	12.9[2.4]
3184.0	4.2[1.2]	24.5[4.6]
3576.0	14.3[4.3]	13.5[2.6]
3402.8	22.4[6.6]	0.0[0.0]
3047.0	5.0[1.5]	13.9[2.6]
3616.0	7.8[2.3]	7.8[1.5]
4-5MeV		
4078.0	14.3[11.4]	6.6[6.3]
4073.1	6.5[5.2]	4.7[4.5]
4265.0	7.5[6.0]	2.2[2.1]
4135.0	3.0[2.4]	5.5[5.2]
4363.9	2.4[1.9]	6.0[5.7]
4227.5	4.3[3.4]	0.0[0.0]

[a] Numbers in square brackets are the percent contribution of each line to the total photo-peak counts in 1MeV bins. For example, we estimate there to be 4967 (experimental) photo-peak counts in the range of 1-2MeV, so the line at $E_\gamma = 1427$keV contributes 13% to the total.The discrepancy between the normalizations for the experiment and MC arise because $\sim 60\%$ of the photon counts come from very weak lines. These lines are counted as part of the "background" in the analysis of experimental data.

Table 2
Fit parameters for s_γ for thermal neutrons on ^{239}Pu.

Energy range(keV)	A_1	τ_1(sec)	A_2	τ_2(sec)	A_3	τ_3(sec)
[500-1000keV]	3.63e+04	2.61	1.85e+04	12.09	3.34e+03	97.73
[1000-1500keV]	1.32e+04	2.34	5.63e+03	12.31	2.13e+03	87.82
[1500-2000keV]	8.12e+03	1.81	3.17e+03	10.35	1.05e+03	69.21
[2000-2500keV]	3.40e+03	0.95	1.04e+03	8.61	7.00e+02	65.43
[2500-3000keV]	3.31e+03	1.08	8.09e+02	7.84	5.52e+02	65.61
[3000-3500keV]	2.10e+03	5.92	1.86e+03	1.39	2.42e+02	61.93
[3500-4000keV]	3.76e+02	3.79	1.46e+02	43.69	1.67e+01	5.47e+06
[4000-4500keV]	1.02e+03	1.25	9.89e+01	10.30	5.55e+01	86.24
[4500-5000keV]	1.78e+02	6.64	2.37e+01	34.24	2.29e+00	2.0e+06
[5000-5500keV]	1.41e+02	6.76	1.72e+01	28.83	2.78e+00	3.5e+07
[5500-6000keV]	2.96e+02	10.21	1.29e+02	18.71	-3.36e+02	13.83

Auspices Statement

This work was performed under the auspices of the U.S. Department of Energy by University of California, Lawrence Livermore National Laboratory under Contract W-7405-Eng-48.